Bioorganic & Medicinal Chemistry 18 (2010) 5988–5994

Contents lists available at ScienceDirect

Bioorganic & Medicinal Chemistry

journal homepage: www.elsevier.com/locate/bmc

The marine sponge metabolite mycothiazole: A novel prototype mitochondrial complex I inhibitor

J. Brian Morgan [a], Fakhri Mahdi [a], Yang Liu [a], Veena Coothankandaswamy [a], Mika B. Jekabsons [b], Tyler A. Johnson [c], Koneni V. Sashidhara [c,†], Phillip Crews [c], Dale G. Nagle [a,d,*], Yu-Dong Zhou [a,*]

[a] Department of Pharmacognosy, School of Pharmacy, University of Mississippi, University, MS 38677, United States
[b] Department of Biology, University of Mississippi, University, MS 38677, United States
[c] Department of Chemistry and Biochemistry, University of California Santa Cruz, Santa Cruz, CA 95064, United States
[d] Research Institute of Pharmaceutical Sciences, University of Mississippi, University, MS 38677, United States

ARTICLE INFO

Article history:
Received 19 May 2010
Revised 18 June 2010
Accepted 21 June 2010
Available online 25 June 2010

Keywords:
Hypoxia-inducible factor-1 (HIF-1)
Marine natural products
Mitochondrial complex I inhibitor
NADH-ubiquinone oxidoreductase

ABSTRACT

A natural product chemistry-based approach was applied to discover small-molecule inhibitors of hypoxia-inducible factor-1 (HIF-1). A *Petrosaspongia mycofijiensis* marine sponge extract yielded mycothiazole (**1**), a solid tumor selective compound with no known mechanism for its cell line-dependent cytotoxic activity. Compound **1** inhibited hypoxic HIF-1 signaling in tumor cells (IC_{50} 1 nM) that correlated with the suppression of hypoxia-stimulated tumor angiogenesis in vitro. However, **1** exhibited pronounced neurotoxicity in vitro. Mechanistic studies revealed that **1** selectively suppresses mitochondrial respiration at complex I (NADH-ubiquinone oxidoreductase). Unlike rotenone, MPP^+, annonaceous acetogenins, piericidin A, and other complex I inhibitors, mycothiazole is a mixed polyketide/peptide-derived compound with a central thiazole moiety. The exquisite potency and structural novelty of **1** suggest that it may serve as a valuable molecular probe for mitochondrial biology and HIF-mediated hypoxic signaling.

1. Introduction

Marine natural products have emerged as a rich source of chemical diversity for drug discovery, especially in the area of molecular-targeted anticancer chemotherapeutics.[1,2] Mycothiazole (**1**) belongs to a structurally distinct class of mixed polyketide synthase/non-ribosomal peptide synthase (PKS-NRPS)-derived natural products that contain a thiazole ring embedded between two acyclic polyketide chains.[3] Mycothiazole was first isolated from the marine sponge *Spongia mycofijiensis*[4] [subsequently reclassified as *Cacospongia mycofijiensis*[5,6] Kakou, Crews, & Bakus (Thorectidae)], and later reported to exhibit tumor cell line-dependent cytotoxicity in the National Cancer Institute (NCI) 60-cell line screen.[7] The structural uniqueness and pharmacological activity of **1** have inspired numerous projects aimed at its total synthesis.[7–15] However, the *E*-configuration at the C-14/C-15 double bond of **1** has recently been revised to *Z*,[3] and no report has appeared describing the total synthesis of this revised scaffold. Furthermore, the molecular target(s) affected by **1** and the mechanism(s) of action for **1** to suppress tumor cells have remained unknown.

2. Results and discussion

2.1. Compound acquisition and HIF-1 inhibitory activity

Mycothiazole (**1**) was obtained during our campaign to discover natural product-derived small molecule HIF-1 inhibitors. A key regulator of oxygen homeostasis, HIF-1 mediates cellular adaptation to hypoxia by activating the expression of genes that increase oxygen availability and those that decrease oxygen consumption.[16] Extensive laboratory and clinical studies indicate that the dysregulation of HIF-1 contributes to both the etiology and progression of cancer.[16] Preclinical studies revealed that HIF-1 inhibition reduces tumor growth/progression and enhances treatment outcome when combined with radiation and chemotherapeutic agents.[16] Over 15,000 extracts of marine invertebrates and algae (NCI's Open Repository) were evaluated in a human breast tumor T47D cell-based reporter assay for HIF-1 inhibitory activity.[17] An active lipid extract of the marine sponge *Petrosaspongia mycofijiensis* inhibited hypoxia (1% O_2)-induced HIF-1 activation by 97% (5.0 μg/mL). Bioassay-guided isolation followed by dereplication-based structure elucidation of **1** employed data from a combination of ^1H and

* Corresponding authors. Tel.: +1 662 915 7026; fax: +1 662 915 6975 (D.G.N.); tel.: +1 662 915 7026; fax: +1 662 915 6975 (Y.-D.Z.).
E-mail addresses: dnagle@olemiss.edu (D.G. Nagle), ydzhou@olemiss.edu (Y.-D. Zhou).
† Present address: Central Drug Research Institute, CSIR, Lucknow 226 001, India.

0968-0896/$ - see front matter © 2010 Elsevier Ltd. All rights reserved.
doi:10.1016/j.bmc.2010.06.072

^{13}C NMR spectroscopy and ESI mass spectrometry. Mycothiazole and two structurally related compounds [8-*O*-acetylmycothiazole (**2**) and 4,19-dihydroxy-4,19-dihydromycothiazole (**3**)] were evaluated in a T47D cell-based reporter assay to determine their effects on HIF-1 activation. Compound **1** blocked hypoxia-induced HIF-1 activation at single-digit nanomolar concentrations (Fig. 1A). In contrast, **1** did not inhibit chemical hypoxia (10 μM 1,10-phenanthroline)-activated HIF-1 at concentrations up to 10 μM (data not shown). Compound **2** exhibited similar HIF-1 inhibitory activity and selectivity as observed for **1** (Fig. 1A). Compound **3** was at least 1000 times less potent than the other two compounds at suppressing hypoxia-induced HIF-1 activation (Fig. 1A).

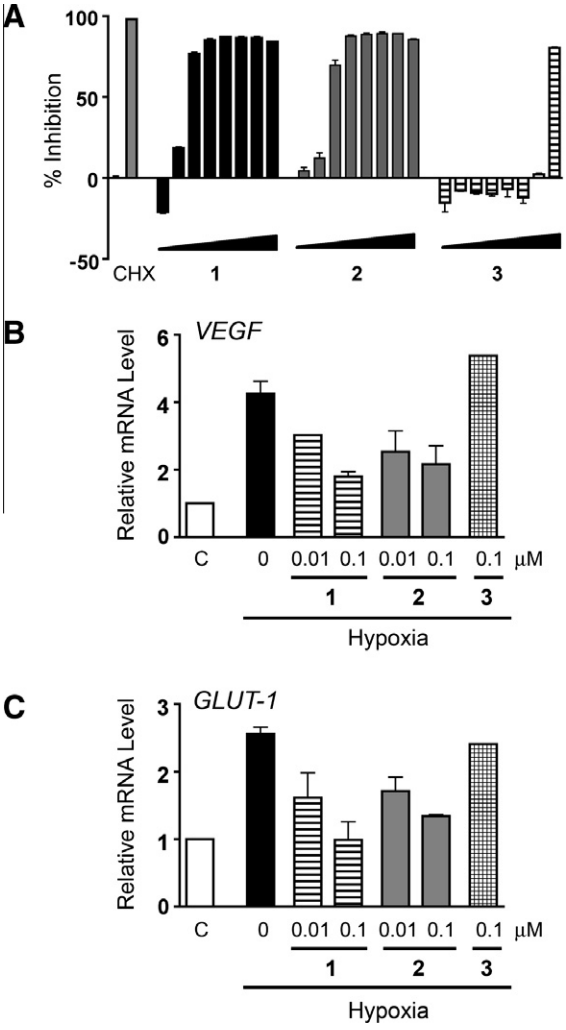

Figure 1. Effects of mycothiazole (**1**) and mycothiazole analogues (**2** and **3**) on hypoxia-induced HIF-1 activation. (A) Concentration-dependent inhibition of hypoxia (1% O_2)-induced HIF-1 activation in a T47D cell-based reporter assay. Compounds **1**–**3** were tested at the incrementing concentrations of 0.1, 0.3, 1, 3, 10, 30, 100, and 1000 nM. The protein synthesis inhibitor cycloheximide (CHX) was tested at 100 μM as a positive control. Data shown are averages from one representative experiment performed in triplicate and the error bars indicate standard deviation. (B) Compounds **1** and **2** inhibited hypoxic induction of *VEGF* mRNA. T47D cells were exposed to hypoxic conditions (1% O_2, 16 h) in the presence and absence of compounds **1**–**3**. Total RNA samples were isolated from the treated and untreated cells. The level of *VEGF* mRNA in each sample was quantified by real time RT-PCR, normalized to an internal control (18S rRNA), and presented as relative mRNA level of the normoxic control (C). Data shown are averages from two independent experiments and the error bars represent deviation from the average. (C) Compounds **1** and **2** inhibited hypoxic induction of *GLUT-1* mRNA. Experimental design and data interpretation were the same as those described in (B) except *GLUT-1* gene-specific primers were used.

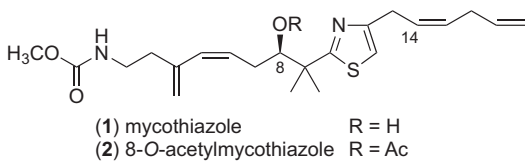

(**1**) mycothiazole R = H
(**2**) 8-*O*-acetylmycothiazole R = Ac

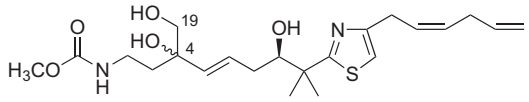

(**3**) 4,19-dihydroxy-4,19-dihydromycothiazole

2.2. Suppression of HIF-1 target gene expression

The effects of **1** and analogues on the hypoxic induction of HIF-1 target genes *VEGF* (vascular endothelial growth factor) and *GLUT-1* (glucose transporter-1) were examined by real time RT-PCR. In T47D cells, hypoxic exposure (1% O_2, 16 h) increased the expression of *VEGF* (Fig. 1B) and *GLUT-1* (Fig. 1C) at the mRNA level. Compounds **1** and **2** both suppressed the hypoxic induction of HIF-1 target genes in a concentration-dependent manner. In contrast, **3** (0.1 μM) did not inhibit the induction of either *VEGF* or *GLUT-1* mRNAs. The effects exerted by these three compounds on the hypoxic induction of endogenous HIF-1 target genes mirror the response observed in the cell-based HIF-1 reporter assay (Fig. 1A).

2.3. Inhibition of hypoxia-induced angiogenesis

Hypoxia represents an important stimulus for tumor angiogenesis. One of the mechanisms employed by hypoxic tumor cells to promote angiogenesis is through the HIF-1-dependent induction of VEGF, a potent angiogenic factor.[18] Agents that inhibit VEGF are in clinical use for cancer.[18] In T47D cells, both hypoxic exposure (1% O_2, 16 h) and iron chelator treatment (10 μM 1,10-phenanthroline, 16 h) significantly increased the production of secreted VEGF protein, relative to the untreated control (Fig. 2A). Compound **1** selectively suppressed the induction of secreted VEGF protein by hypoxia, relative to its effect on 1,10-phenanthroline-induced VEGF (Fig. 2A). To assess the anti-angiogenic potential of **1**, a human umbilical vein endothelial cell (HUVEC)-based tube formation assay was employed as an in vitro model. In the absence of angiogenic signals, HUVEC cells appear scattered (Fig. 2Ba). Addition of angiogenic factors (e.g., recombinant human VEGF protein) stimulated HUVEC cells to form interconnected tube-like structures (tube formation).[19] Normoxic T47D cell-conditioned media also induced tube formation (Fig. 2Bb). Hypoxic exposure (1% O_2, 16 h) significantly enhanced the angiogenic activity of the T47D cell-conditioned media sample (Fig. 2Bd), most likely through increased production of angiogenic factors such as VEGF. At the concentration that inhibited hypoxia-induced HIF-1 activation and VEGF induction, **1** (10 nM) suppressed the angiogenic activity of the hypoxic T47D cell-conditioned media (Fig. 2Be). This inhibitory effect was specific for hypoxic inducing conditions. Compound **1** did not inhibit the ability of normoxic T47D cell-conditioned media to induce angiogenesis (Fig. 2Bc). The observation that **1** did not inhibit tube formation when added to the hypoxic T47D cell-conditioned media sample (Fig. 2Bf) suggested that **1** inhibits tumor angiogenesis by blocking the expression of angiogenic factors, not by directly suppressing the tube formation process. Quantification results (Fig. 2C, tube length; Fig. 2D, number of branching points) corroborate the microscopic observations (Fig. 2B).

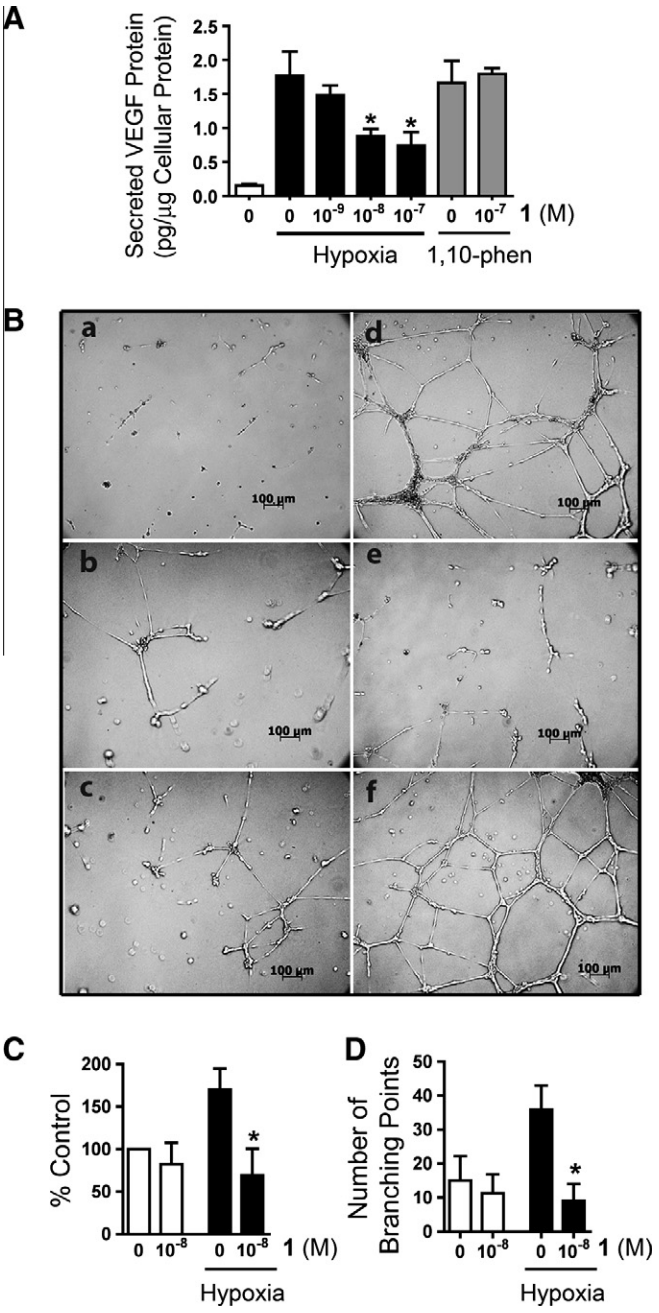

Figure 2. Mycothiazole (**1**) inhibits hypoxic induction of secreted VEGF protein and tumor angiogenesis in vitro. (A) T47D cells were exposed to hypoxia (1% O_2) or 1,10-phenanthroline (10 μM) in the presence and absence of **1** for 16 h. Levels of secreted VEGF protein in the T47D cell-conditioned media samples were determined by ELISA and normalized to the amounts of cellular proteins. Data shown are average + standard deviation ($N = 3$). An asterisk (*) indicates $p < 0.05$ when compared to the induced control using one-way ANOVA and Bonfferoni post hoc analyses (GraphPad Prism 4). (B) The effects of T47D cell-conditioned media samples on tumor angiogenesis were evaluated in a HUVEC-based tube formation assay. Representative images are shown and each panel includes a 100 μm scale bar. The panels are: (a) basal media (negative control); (b) normoxic T47D cell-conditioned media; (c) **1** (10 nM) treated normoxic T47D cell-conditioned media; (d) hypoxic T47D cell-conditioned media; (e) **1** (10 nM) treated hypoxic T47D cell-conditioned media; and (f) hypoxic T47D cell-conditioned media and **1**. (C) Relative tube length in three randomly selected fields for conditions in Fig. 3B (b–e). The data shown are averages and the error bars indicate standard deviation. An asterisk (*) indicates a statistically significant difference ($p < 0.05$) between the hypoxic control and mycothiazole treated hypoxic samples. (D) Experimental conditions and data presentation are the same as those described in (C) except the number of branching points was quantified as the tube formation parameter.

2.4. Mechanism of action studies

2.4.1. HIF-1α expression

Discerning the mechanism of action for **1** to inhibit HIF-1 activation involved a multi-step process. We first examined the effect of **1** on the induction of nuclear HIF-1α protein in T47D cells. In general, the induction and activation of the oxygen-regulated HIF-1α subunit determines HIF-1 activity.[20] Under normoxic conditions, HIF-1α protein was absent in the nuclear extract sample from control cells (Fig. 3A). Exposure to hypoxic conditions (1% O_2, 4 h) induced the accumulation of nuclear HIF-1α protein (Fig. 3A). While the relative potency was superficially diminished by the short incubation time course (Western blot 4 h; pHRE3-TK-Luc reporter assay 16 h), **1** blocked the hypoxic induction of HIF-1α protein in the nucleus. In contrast, the levels of the constitutively expressed HIF-1β subunit in the nuclear extract samples were not affected (Fig. 3A). Compounds that disrupt the mitochondrial electron transport chain (ETC) have been shown to selectively suppress hypoxia-induced HIF-1 activation.[1,21]

2.4.2. Mitochondrial respiration studies

To investigate if **1** inhibits mitochondrial function, a T47D cell-based respiration study was performed.[19] Compound **1** suppressed oxygen consumption in a concentration-dependent manner (Fig. 3B). The effective concentrations for **1** to suppress oxygen consumption were within the range of the concentrations required to inhibit hypoxia-induced HIF-1 activation. Further mechanistic studies were performed to discern the specific site within the mitochondrial ETC that is affected by **1**. The first study was to investigate if **1** acts as an inhibitor of complex II, III, or IV of the ETC (Fig. 3C). Addition of a mixture of malate and pyruvate to digitonin-permeabilized T47D cells started respiration by initiating NADH production, thereby providing a source of electrons for complex I (NADH-ubiquinone oxidoreductase). The electrons then pass through a series of electron carriers along the ETC to oxygen, the end electron acceptor. The level of respiration correlates with the rate of oxygen consumption. Complex I inhibitors such as rotenone (**4**) suppressed respiration, reflected by a dramatic decrease in oxygen consumption rate (Fig. 3C). Succinate overcame complex I inhibitor-imposed respiration blockade by providing electrons to complex II (succinate-ubiquinone oxidoreductase) of the respiratory chain. The observation that **1** (10 and 30 nM) failed to inhibit respiration in the presence of succinate suggests that **1** does not inhibit complex II, III, or IV (Fig. 3C). In contrast, antimycin A (**5**) [an inhibitor of complex III (ubiquinol-cytochrome c oxidoreductase)] suppressed respiration in the presence of succinate. A mixture of ascorbate and TMPD (*N*,*N*,*N*′,*N*′-tetramethyl-*p*-phenylenediamine) that serves as an electron source for cytochrome c and hence for complex IV (cytochrome c oxidase) caused a resumption of respiration that was otherwise blocked at complex III. These observations suggest that **1** does not affect complexes II, III, or IV of the ETC. To test the hypothesis that **1** inhibits mitochondrial respiration by selectively targeting complex I, **1** (10 nM) was added to permeabilized T47D cells following the initiation of respiration by a mixture of malate/pyruvate. Compound **1** suppressed respiration and this inhibition was subsequently overcome by the complex II substrate succinate (Fig. 3D). These data indicate that **1** suppresses mitochondrial respiration by selectively inhibiting ETC complex I.

The effects of **1**–**3** on cellular respiration were further examined in a T47D cell-based concentration-response study and the data compared to the complex I inhibitor rotenone (**4**) (Fig. 3E). Compound **1** is more potent than **4** at suppressing cellular respiration in T47D cells. Although **1** and **2** exhibited comparable HIF-1 inhibitory activities, **2** was at least 3-times less potent. One possible explanation may be that **1** is the active inhibitor and ester

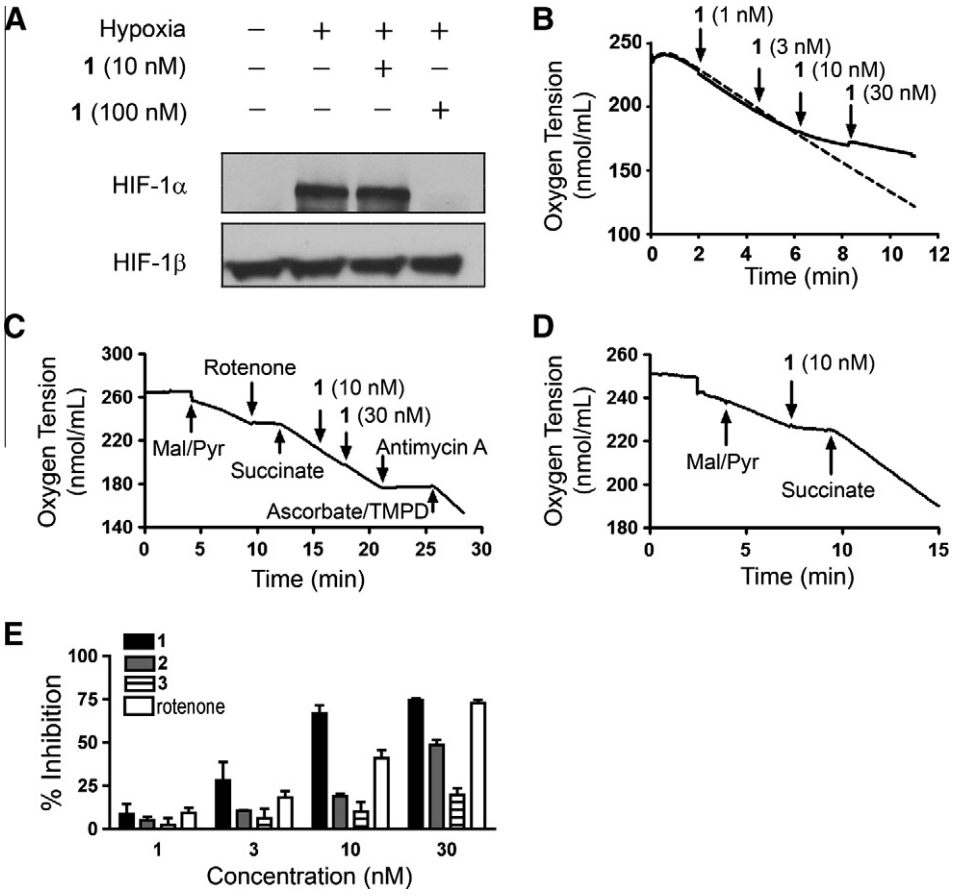

Figure 3. Mycothiazole inhibits hypoxic induction of nuclear HIF-1α protein and suppresses mitochondrial respiration at low nanomolar concentrations. (A) Western blot analysis was performed to determine the levels of HIF-1α and HIF-1β proteins in nuclear extract samples prepared from T47D cells exposed to hypoxia (1% O_2, 4 h) in the presence and absence of mycothiazole (**1**). (B) Mycothiazole (**1**) inhibited oxygen consumption in T47D cells in a concentration-dependent manner (solid line). Oxygen consumption in control cells is shown as a dotted line. (C) Compound **1** did not affect mitochondrial ETC complex II, III, or IV. Substrates and inhibitors were added to digitonin (10 μM)-permeabilized T47D cells at the specified time point in a sequential manner. (D) Compound **1** inhibited mitochondrial respiration by targeting complex I. (E) Effects of mycothiazole (**1**), 8-*O*-acetylmycothiazole (**2**), and 4,19-dihydroxy-4,19-dihydromycothiazole (**3**) on T47D cell oxygen consumption. Compounds **1** (black bar), **2** (gray bar), **3** (striped bar) and a positive control rotenone (**4**) (open bar) were tested at the specified concentrations. Data are presented as% Inhibition relative to the untreated control. Averages from three independent experiments are shown and the error bars represent standard deviation.

hydrolysis of **2** requires significantly longer cellular incubation than that used for the respiration studies. As anticipated, the least active HIF-1 inhibitor **3** (30 nM) did not significantly inhibit cellular respiration.

2.5. Tumor cell proliferation/viability

Cell line-dependent growth inhibitory effects were observed when mycothiazole was examined in the NCI-60 cell line study.[4] However, many of the cell lines were insensitive to **1** treatment (GI_{50} >30 μM, TGI and LC_{50} >100 μM). The finding that **1** inhibited mitochondrial respiration at complex I would tend to indicate that the effects of **1** and related compounds on cell proliferation/viability be reexamined. Standard cytostatic/cytotoxic assays are generally performed following a 48 h compound treatment/incubation period. McLaughlin and colleagues reported that an extended exposure time (i.e., 6 d) is required for mitochondrial inhibitors to suppress cell proliferation/viability.[22] Six-day concentration-response studies were performed to determine the effects of mycothiazole and the two analogues on tumor cell proliferation/viability. The inhibitory effects exerted by these compounds on tumor cell proliferation/viability parallel those observed in the reporter assay for HIF-1 activity. Compounds **1** and **2** suppressed cell proliferation/viability with comparable potency, while **3** was at least three orders of magnitude less active (Fig. 4A–C). Among the cell lines examined, T47D cells were the most sensitive and MDA-MB-231 cells were the least sensitive. The observation that the level of inhibition plateaued at 55% in T47D cells suggests that only a subpopulation of cells were sensitive to **1** and **2**.

2.6. Neurotoxicity

One of the potential side effects associated with the application of mitochondrial inhibitors is neurotoxicity.[22] Primary rat cerebellar granule neurons (CGNs) were used as an in vitro model for neurotoxicity. Following 24 h compound treatment, the cells were stained with propidium iodide and Hoechst-33342. Because propidium iodide does not penetrate cell membranes, it stains only dead cells. Based on morphological characteristics, the cells were counted and grouped (live versus dead, Fig. 4E; dead neurons—apoptotic, early stage necrotic, and propidium iodide positive, Fig. 4F). Compound **1** (10 nM, 24 h) treatment killed all the cells (Fig. 4D and E). Compound **1** was more toxic than the positive control rotenone that was tested at a ten times higher concentration (Fig. 4D and E). Detachment of the dead cells contributed to the decrease in the total number of rotenone treated cells (Fig. 4E). Approximately 60% of the attached dead neurons following rotenone treatment exhibited apoptotic morphology, while 85% of the neurons killed by **1** were late stage apoptotic/necrotic (Fig. 4F).

3. Conclusion

Mitochondria consume over 90% of the cellular oxygen through oxidative phosphorylation to produce ATP. The hypoxia-ROS-HIF model proposes that hypoxia increases mitochondrial ROS and that the ROS provide a signal that stabilizes HIF-1α protein and activates HIF-1.[21] This study characterized the effects of mycothiazole (**1**) on HIF-1 signaling pathway and established a probable mechanism of action for the bioactivities observed for **1**. Compound **1** represents the first member of a structurally novel class of mitochondrial ETC complex I inhibitors. Because of its structural uniqueness, **1** may interact with the large 45 polypeptide complex I complex at a site different from other natural product-based [rotenone (**4**), piericidin (**6**), annonacin (**7**), capsaicin (**8**), etc.] and synthetic complex I inhibitors [phenoxan (**9**), fenpyroximate (**10**), MPP^+ (**11**), and pyridaben (**12**)].[23] The superficial structural resemblance of **1** to the complex III inhibitor myxothiazole (**13**) further highlights the novelty of this selective complex I inhibitor as a potentially valuable molecular probe to investigate mitochondrial function and hypoxic signaling.

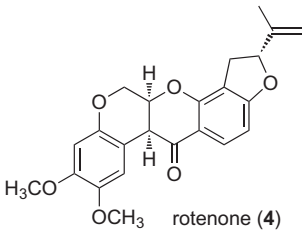

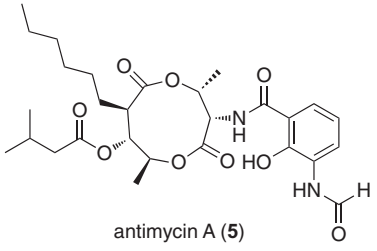

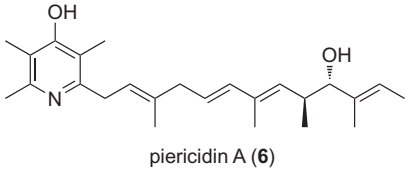

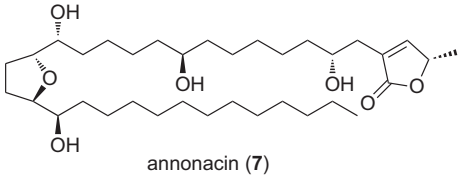

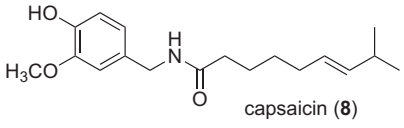

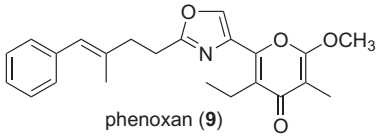

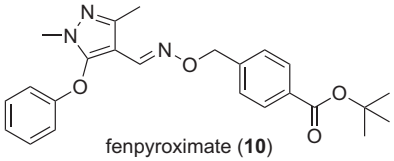

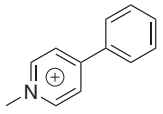

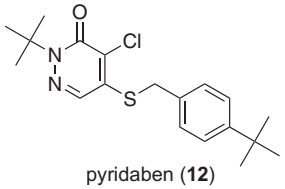

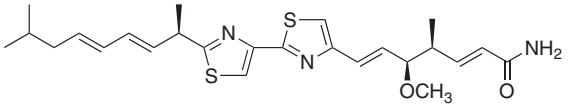

4. Experimental section

4.1. Sponge material, extraction, and isolation

The sponge material (C021045) was obtained from the National Cancer Institute's Open Repository Program. *Petrosaspongia mycofijiensis* Bakus (Thorectidae) was collected from underwater caves (−20 m depth) off the coast of Vanuatu by Dr. Patrick L. Colin (Coral Reef Research Foundation) on November 18, 2000. The sample was identified by Dr. Michelle Kelly (National Institute of Water and Atmospheric Research Limited, Auckland, New Zealand). Marine sponge taxonomy is vibrant and ever changing. Our experience would indicate that samples of the mycothizole-producing sponge identified as *P. mycofijiensis* and the original samples of *Cacospongia mycofijiensis* are the same species of sponge found in the waters off Vanuatu. A voucher specimen of the sample used to generate the extract for the NCI Open Repository was placed on file with the Department of Invertebrate Zoology, National Museum of Natural History, Smithsonian Institution, Washington, D.C. The sponge material was frozen at −20 °C, ground in a meat grinder, and extracted with water. The residual material was lyophilized and extracted with CH_2Cl_2/MeOH (1:1), solvents removed under vacuum, and the crude extract stored -20 °C in the NCI's Open Repository at the Frederick Cancer Research and Development Center (Frederick, Maryland). The crude extract (3.0 g) was subjected to bioassay-guided standard Si gel (200–400 mesh) column chromatography analysis that yielded **1** (41.4 mg). The NMR spectra were recorded in $CDCl_3$ on Bruker AMX-NMR spectrometers operating at either 400 MHz or 600 MHz for ^1H and either 100 MHz or 150 MHz for ^{13}C, respectively. The NMR spectra were recorded running gradients and residual solvent peaks (δ 7.27 for ^1H) and (δ 77.0 for ^{13}C) were used as internal references. The data matched those of mycothiazole.[3] Compound **2** was obtained by semi-synthesis. A sample of **1** (5 mg, isolated from *C. mycofijiensis*) was dissolved in dry

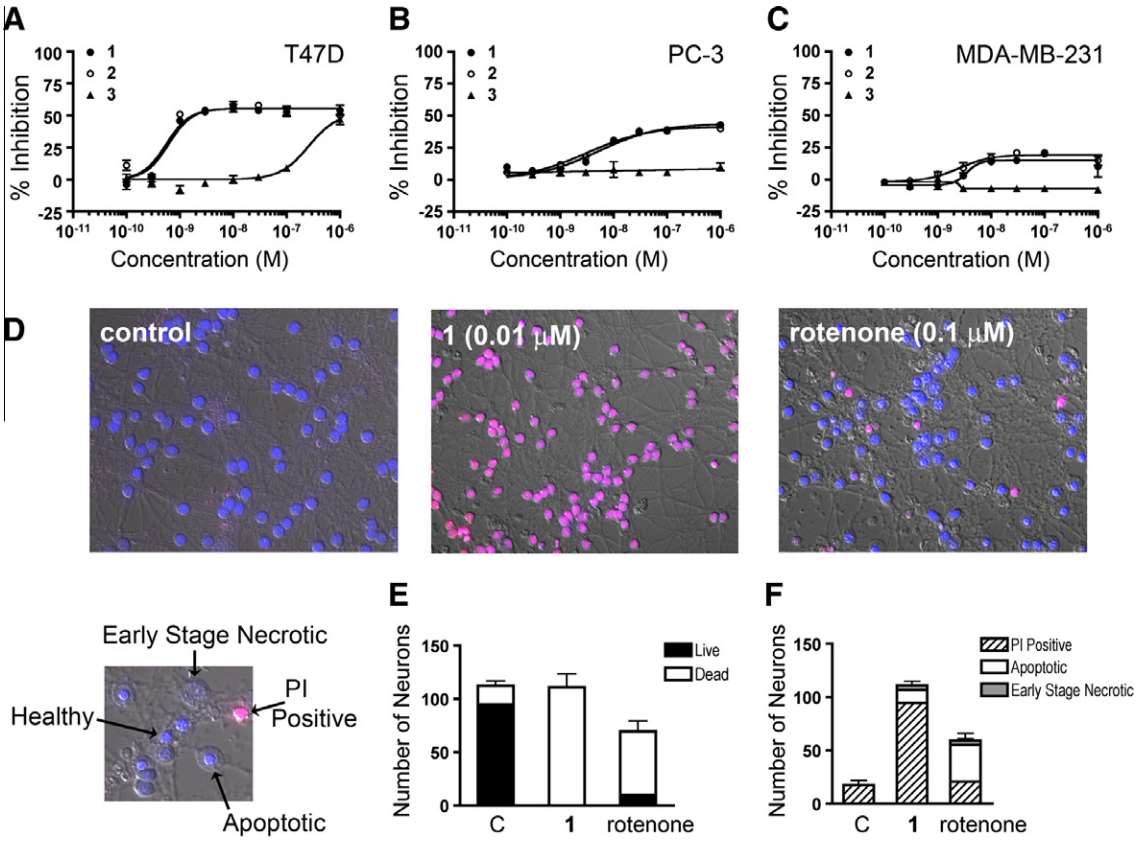

Figure 4. Cell line-dependent growth inhibition and cytotoxicity by mycothiazole and analogues. Six-day concentration–response results of mycothiazole (**1**), 8-*O*-acetylmycothiazole (**2**), and 4,19-dihydroxy-4,19-dihydromycothiazole (**3**) on the proliferation/viability of T47D (A), PC-3 (B), and MDA-MB-231 (C) cells. Cell viability was determined using the sulforhodamine B method and presented as %inhibition of the untreated control. Data are averages from one representative experiment performed in triplicate and the error bars represent standard deviation. (D) Representative images of untreated rat cerebellar granule neurons (CGNs, control) and those exposed to rotenone (**4**, 0.1 μM) and **1** (0.01 μM), stained with Hoescht 33342 and propidium iodide (PI). (E) The extent of cell death in four randomly selected fields was quantified for each condition in D, according to the morphologic characteristics defined in the panel to the left. CGNs that exhibited the characteristics of apoptotic (PI negative, condensed or fragmented nuclei), early stage necrotic (PI negative, fragmented nuclei, and swelled morphology), necrotic and late stage apoptotic (PI positive) cells are all considered dead or dying. The PI negative and healthy cells are grouped as live. Averages from one representative experiment (out of three experiments) are shown and the bars indicate standard deviation. (F) The dead or dying CGNs observed in D were grouped as apoptotic, early stage necrotic, and PI positive (necrotic and late stage apoptotic). Data presentation was the same as described in E.

pyridine (300 μL) and acetic anhydride (1000 μL). The mixture was stirred for 24 h and the reaction was quenched with water and extracted with CH_2Cl_2. The organic layer was dried with $NaSO_4$ and purified using RP-HPLC (Phenomenex Luna 5μ, C_{18} (2), 250 × 10.00 mm, isocratic 70% CH_3CN in H_2O, 2.0 mL/min) to generate **2** (1.7 mg). Compound **3** was purified from a 2002 collection of an individual *C. mycofijiensis* specimen from Vanuatu (collection no. 02600, 12.7 g wet weight). The sample was soaked in MeOH (24 h) and partitioned as described previously.[3,6] The CH_2Cl_2 extract (11.9 mg) was purified using HPLC (10:90→100% CH_3CN, 30 min) to yield pure **1** (3.1 mg) and **3** (1.8 mg). The spectroscopic and spectrometric properties of **1** and **3** were as previously described.[3]

4.1.1. 8-*O*-Acetylmycothiazole (2)

white oil; $[\alpha]_D^{24}$ −7.0 (*c* 0.1, MeOH); UV (MeOH) λ_{max} (log ε): 233.4 nm (3.7); ^{1}H NMR ($CDCl_3$, 600 MHz) δ 5.83 (1H, ddt, *J* = 16.2, 10.2, 6.0, H-17), 5.77 (1H, br d, *J* = 12.2, H-5), 5.72 (1H, dtt, *J* = 10.2, 7.2, 1.2, H-14), 5.60 (1H, dtt, *J* = 10.2, 7.8, 1.8, H-15), 5.41 (1H, ddd, *J* = 11.4, 8.4, 6.0, H-6), 5.30 (1H, dd, *J* = 10.2, 3.0, H-8), 5.07 (1H, dq, *J* = 17.4, 1.8, H-18), 5.00 (1H, dq, *J* = 10.2, 1.8, H-18′), 4.97 (1H, br s, H-19), 4.80, (1H, br s, H-19′), 3.65 (3H, s, OMe), 3.55 (1H, d, *J* = 7.2, H-13), 3.24 (1H, dddd, *J* = 13.8, 7.2, 6.6, 6.0, H-2), 3.16 (1H, dddd, *J* = 13.8, 8.4, 6.0, 4.8, H-2), 2.89 (2H, ddd, *J* = 7.8, 3.6, 1.8, H-16), 2.48 (1H, dddd, *J* = 15.0, 10.2, 8.4, 1.2, H-7), 2.35 (1H, m, H-7′), 2.25 (1H, m, H-3), 2.02 (3H, s, OAc), 1.43, (3H, s, H_3-20), 1.42 (3H, s, H_3-21); ^{13}C NMR detected indirectly by HMQC and HMBC (see Supplementary data) ($CDCl_3$ 150 MHz) δ 179.4 (C, C-10), 156.6 (C, C-1), 154.9 (C, C-12), 142.2 (C, C-4), 131.9 (CH, C-5), 129.2 (CH, C-6), 128.4 (CH, C-15), 127.9 (CH, C-14), 125.3 (CH, C-17), 115.9 (CH_2, C-19), 115.2 (CH_2, C-18), 112.5 (CH, C-11), 79.4 (CH, C-8), 51.2 (CH_3, OMe), 44.5 (C, C-9), 39.9 (CH_2, C-2), 37.1 (CH_2, C-3), 31.4 (CH_2, C-16), 30.7 (CH_2, C-7), 29.4 (CH_2, C-13), 26.1 (CH_3, Me-20), 23.9 (CH_3, Me-21), 20.9 (CH_3, OAc); HRESI-MS $[M+Na]^+$ *m/z* 469.2123 (calcd for $C_{24}H_{34}N_2O_4NaS$, 469.2157).

4.1.2. Stabilization and formulation

The integrity of **1** was monitored by thin-layer chromatography (TLC) analysis using Merck $Si_{60}F_{254}$ plates, visualized after spraying with a 1% (v/v) anisaldehyde solution in AcOH/H_2SO_4 (50:1) and subsequent heating. The stock solution of stabilized **1** contains a mixture of **1** (2 mM) and EDTA (3 mM) in DMSO. In general, either freshly prepared **1** or the stabilized **1** was used for bioassays.

4.2. Biological studies

4.2.1. Cell culture and cell-based reporter and viability assays

Human breast tumor T47D cells (ATCC) were maintained in DMEM/F12 media with L-glutamine (Mediatech), supplemented

with 10% (v/v) fetal bovine serum (FBS, Hyclone), 50 units/mL penicillin and 50 μg/mL streptomycin (Lonza). To monitor HIF-1 activity, a cell-based luciferase assay employing the pHRE3-TK-Luc reporter was performed as described.[17] The sulfarhodamine B method was used to determine cell viability.[19] For the six-day exposure study, the conditioned media were replaced by fresh culture medium that contains test compound after three days.

4.2.2. RNA extraction and quantitative real-time RT-PCR

The plating of T47D cells, compound treatment, extraction of total RNA samples, synthesis of the first strand cDNAs, gene-specific primer sequences, quantitative real-time PCR reactions, and data analysis were described.[19]

4.2.3. ELISA assay for human VEGF protein

The plating of T47D cells, compound treatments, and ELISA assay for secreted and cellular VEGF proteins were described.[17] The concentration of proteins in the cellular lysate was determined using a micro BCA assay (PIERCE), and the amount of VEGF protein was normalized to that of proteins in the cellular lysate.

4.2.4. HUVEC-based tube formation assay

The maintenance of HUVEC cells (Lonza), collection of T47D cell-conditioned media (CM) samples, the performance and quantitation of the HUVEC-based in vitro tube formation assay were described previously.[19]

4.2.5. Nuclear extract preparation and Western blot analysis

Plating of T47D cells, compound treatment, and exposure to hypoxic conditions were described.[17] Nuclear extract preparation using NE-PER nuclear and cytoplasmic extraction kit (PIERCE), and determination of the levels of HIF-1α and HIF-1β proteins in the nuclear extract samples by Western blot were described previously.[19]

4.2.6. Mitochondria respiration assay

An Oxytherm Clarke-type electrode System (Hansatech) was used to monitor the rate of oxygen consumption in T47D cells. A non-permeabilized cell-based respiration assay was performed to determine the effects of purified compounds on cellular respiration.[19] Mechanistic studies were conducted in plasma membrane permeabilized cells to manipulate the mitochondrial substrates and inhibitors. Detailed experimental procedures and reagents were the same as those described.[19]

4.2.7. Cerebellar granule neuron preparation and neurotoxicity assay

Isolation and maintenance of cerebellar granule neurons (CGNs) from the cerebella of rat pups (6–7 day old Wistar, Harlan) were performed as described.[24] The cells were plated onto polyethyleneimine-coated LabTek II chamber slides (8-well format, 0.6×10^6 cells per well) and maintained at 37 °C in a humidified 95% air/5% CO_2 environment. Neurotoxicity assays were conducted in cells that had been in culture for 6–10 days. The cells were exposed to test compounds at specified concentrations for 24 h. At the end of incubation, the cells were washed once with buffer A (116 mM NaCl, 25 mM KCl, 20 mM TES, 10 mM glucose, 1.3 mM $CaCl_2$, 1.3 mM $MgCl_2$, 1.2 mM Na_2SO_4, 0.4 mM KH_2PO_4, 0.2 mM $NaHCO_3$, pH 7.3), and stained for 20 min in buffer A supplemented with 5 μg/mL Hoescht 33342 and 1 μg/mL propidium iodide. The chemicals were purchased from Sigma. The cells were imaged with an Axiovert 200 M epifluorescent microscope and 40× fluar oil objective (Zeiss). Random fields were imaged so that at least 100 cells per treatment per experiment were obtained. Propidium iodide positive cells were scored as late stage apoptotic/necrotic. The propidium iodide-negative cells with condensed and/or fragmented nuclei (as indicated by Hoescht staining) were scored as apoptotic. The propidium iodide-negative cells with swelled and fragmented nuclei were scored as early stage necrotic.

4.2.8. Statistical analysis

Data were compared using one-way ANOVA followed by Bonfferoni post hoc analyses (GraphPad Prism 4). Differences were considered statistically significant when $p < 0.05$.

Acknowledgements

The authors thank S.L. McKnight (UT Southwestern Medical Center at Dallas) for the pHRE-TK-luc construct, D.J. Newman and E.C. Brown (Natural Products Branch Repository Program, NCI—Frederick) for providing marine extracts and collection information. This research was supported in part, by NIH Grants CA98787, P20RR021929, CA047135, NOAA/NIUST Grant NA16 RU1496, and a Government of India BOYSCAST fellowship (K.V.S.). The work at the University of Mississippi was conducted in a facility constructed with NIH Research Facilities Improvement Grant C06 RR-14503-01.

Supplementary data

Supplementary data associated with this article can be found, in the online version, at doi:10.1016/j.bmc.2010.06.072.

References and notes

1. Nagle, D. G.; Zhou, Y.-D. *Phytochem. Rev.* **2009**, *8*, 415.
2. Sashidhara, K. V.; White, K. N.; Crews, P. *J. Nat. Prod.* **2009**, *72*, 588.
3. Sonnenschein, R. N.; Johnson, T. A.; Tenney, K.; Valeriote, F. A.; Crews, P. *J. Nat. Prod.* **2006**, *69*, 145.
4. Crews, P.; Kakou, Y.; Quinoa, E. *J. Am. Chem. Soc.* **1988**, *110*, 4365.
5. Sanders, M. L.; van Soest, R. W. M. *Biologie* **1996**, *88*, 117.
6. Johnson, T. A.; Tenney, K.; Cichewicz, R. H.; Morinaka, B. I.; White, K. N.; Amagata, T.; Subramanian, B.; Media, J.; Mooberry, S. L.; Valeriote, F. A.; Crews, P. *J. Med. Chem.* **2007**, *50*, 3795.
7. Sugiyama, H.; Yokokawa, F.; Shioiri, T. *Tetrahedron* **2003**, *59*, 6579.
8. Sugiyama, H.; Yokokawa, F.; Shioiri, T. *Org. Lett.* **2000**, *2*, 2149.
9. Rodriguez-Conesa, S.; Candal, P.; Jimenez, C.; Rodriguez, J. *Tetrahedron Lett.* **2001**, *42*, 6699.
10. Le Flohic, A.; Meyer, C.; Cossy, J. *Org. Lett.* **2005**, *7*, 339.
11. Mahler, G.; Serra, G.; Manta, E. *Synth. Commun.* **2005**, *35*, 1481.
12. Le Flohic, A.; Meyer, C.; Cossy, J. *Tetrahedron* **2006**, *62*, 9017.
13. Mahler, G.; Serra, G.; Dematteis, S.; Saldana, J.; Dominguez, L.; Manta, E. *Bioorg. Med. Chem. Lett.* **2006**, *16*, 1309.
14. Amans, D.; Le Flohic, A.; Bellosta, V.; Meyer, C.; Cossy, J. *Pure Appl. Chem.* **2007**, *79*, 677.
15. Rega, M.; Candal, P.; Jimenez, C.; Rodriguez, J. *Eur. J. Org. Chem.* **2007**, *6*, 934.
16. Semenza, G. L. *Curr. Pharm. Des.* **2009**, *15*, 3839.
17. Hodges, T. W.; Hossain, C. F.; Kim, Y. P.; Zhou, Y.-D.; Nagle, D. G. *J. Nat. Prod.* **2004**, *67*, 767.
18. Ferrara, N.; Mass, R. D.; Campa, C.; Kim, R. *Annu. Rev. Med.* **2007**, *58*, 491.
19. Liu, Y.; Veena, C. K.; Morgan, J. B.; Mohammed, K. A.; Jekabsons, M. B.; Nagle, D. G.; Zhou, Y.-D. *J. Biol. Chem.* **2009**, *284*, 5859.
20. Wang, G. L.; Jiang, B. H.; Rue, E. A.; Semenza, G. L. *Proc. Natl. Acad. Sci. U.S.A.* **1995**, *92*, 5510.
21. Klimova, T.; Chandel, N. S. *Cell Death Differ.* **2008**, *15*, 660.
22. McLaughlin, J. L. *J. Nat. Prod.* **2008**, *71*, 1311.
23. Hollerhage, M.; Matusch, A.; Champy, P.; Lombes, A.; Ruberg, M.; Oertel, W. H.; Hoglinger, G. U. *Exp. Neurol.* **2009**, *220*, 133.
24. Jekabsons, M. B.; Nicholls, D. G. *Cell Death Differ.* **2006**, *13*, 1595.